Line Protection Challenges and Its Mitigation in a New Grid Scenario

Jaisaikiran reddy Kurre
Department of Electrical Engineering
IIT Kharagpur
Kharagpur, India
jaisaikiranreddy.kurre@outlook.com

Subhadeep Paladhi
Department of Electrical Engineering
IIT Kharagpur
Kharagpur, India
paladhisubha91@gmail.com

Ashok Kumar Pradhan
Department of Electrical Engineering
IIT Kharagpur
Kharagpur, India
akpradhan@ee.iitkgp.ac.in

***Abstract*—A noticeable transformation in the power network fault characteristics is being observed with the large-scale integration of renewable sources. Control operations associated with renewable plant interfacing converters challenge the available line protection schemes, especially for lines integrating such sources to the grid. Such an issue with available distance protection for lines interconnecting renewable sources is addressed here with a solution, especially for zone-1 operation. Two indices are formulated in the proposed method using local end current and voltage data to ensure correct zone-1 decision. Proposed method is assessed for its performance for different fault situations in a 39-bus New England system with renewable integration and the results are accurate. Comparative analysis with conventional distance protection schemes indicates the strength of the proposed method.**

***Index Terms*—Power system fault, distance relay, zone-1 operation, renewable integration, digital relaying.**

I. Introduction

Present environmental concern compels the power grids to integrate renewable sources in large scale [1]. Fault-ride-though compliance of the grid codes makes the renewable plants not to disconnect from the system even during faults at high voltage levels [2]. Presence of such plants with numerous converter control options regulates the current and voltage signals significantly during fault [3]. Such changes in fault characteristics ask to revisit the performance of available network protection schemes in such a new grid scenario [4], [5]. Distance relaying being the main protection option for transmission networks today, its performance is revisited here for lines connecting renewable sources.

Distance relaying in renewable integrated power network is analyzed in [6]. Performance of the distance relay at the renewable connected substation is found to be limited due to fault current limitation and significant phase angle modulation by the renewable plant interfacing converters [7]. Different approaches are proposed to improve the performance of relay in such circumstances. Adaptive setting methods for distance relay are proposed in [6] for wind farm connected lines require the information on wind speed data and number of participating units. These are acquired using communication links, which results in delay in protection. Local information based adaptive zone-1 setting methods, proposed in [8], [9], for dynamic source impedance variation do not address the issue when converter interfaced sources are present. Relays with multiple zone-setting options for different source impedance ratio (SIR) conditions may not be suitable for instantaneous protection in case of zone-1 faults [10], [11]. Considering the equivalent impedance of sources at both the ends of the power line which is protected to be small and homogeneous, adaptive techniques have been proposed in [12], [13] for compensation of fault resistance effect under the remote infeed presence. Such considerations are not true for a renewable integrated network. Communication based schemes are preferred in [14] for lines with such connectivity. Latency issue associated with such approaches results in delay in protection. A delayed distance relaying decision is recommended in [15] for the power network integrating converter-interfaced renewable plants (CIRPs), for the lines interconnecting them subjected to the remote end relay to be operated correctly. A control strategy is proposed in [7] to maintain homogeneity in the system and prevent distance relay maloperation. It is difficult to generalize such a technique for power systems with different types of renewable plants. Adaptive distance protection methods, proposed in [4], derive correct decisions for zone-1 faults, but do not address the performance in maintaining security against out-of-zone faults.

In this work an approach for zone-1 protection is proposed for lines interconnecting renewable plants to mitigate the problems associated with conventional distance relays. It estimates the angle of current in faulted loop by computing sequence impedances of the renewable plant considering pure fault model continuously regardless of the control schemes associated with it. Two indices are formulated using the phase angle information and are updated with new samples of current and voltage obtained at the relay. The method confirms a zone-1 fault when both the indices are positive and the second index is greater than the first index. The method that is proposed is checked for its performance for various fault conditions on New England modified 39-bus system integrated by renewable sources using the data from PSCAD/EMTDC simulation. Assessment of the proposed method and conventional distance protection scheme comparatively verifies the superiority of the suggested method.

978-1-6654-2873-6/21/$31.00 © 2021 IEEE

II. Distance Protection Challenges in the Presence of Renewable Sources

A two bus equivalent diagram of a power system is shown in Fig. 1 . A renewable plant, modeled by a controlled current source, is integrated at bus M. Z_S, Z_{RN}, and Z_R are the equivalent impedances of the three sources in the diagram. Z_{Tr} is the equivalent impedance of transformer integrating the renewable source.Positive, negative and zero sequence components are represented by 1, 2 and 0 in the subscripts respectively. Z_{MN} is the impedance of the line MN .From bus M at x pu distance a fault is considered with a fault resistance, R_F.

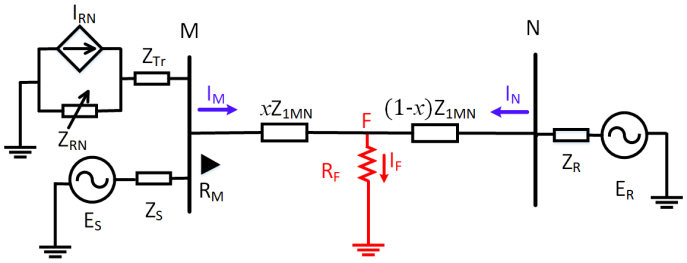

Fig. 1. Two bus equivalent of a CIRP integrated network.

Apparent impedance calculated by the distance relay at bus M (R_M) is given by (1) [4].

$$Z_{app} = \frac{V_{R_M}}{I_{R_M}} = xZ_{1MN} + \left(\frac{I_F}{I_{R_M}}\right) R_F = xZ_{1MN} + \Delta Z \quad (1)$$

where, I_{R_M} and V_{R_M} are the operating current and voltage for the relay, R_M. I_F represents the faulted path current. I_{R_M} gets modulated significantly due to the control operation in renewable plant. High magnitude of $\left(\frac{I_F}{I_{R_M}}\right)$ with large angle difference between I_F and I_{R_M} deviates Z_{app} significantly from actual faulted section impedance and results in distance relay maloperation at times.

Such limited performance of distance relay is demonstrated below as shown in Fig. 2 for a renewable integrated modified New England 39-bus sytem of 345 kV, 60 Hz [16]. PSCAD is used for simulation. Using 1-cycle DFT current and voltage phasors are estimated with samples taken at 3.84 kHz. A solar photovoltaic (PV) source of 300 MW is connected at bus 37 replaces the generator connected at the same bus. The solar plant is modelled by multiple PV units,integrated into the network to the bus (37) through inverter and transformer arrangements [17]. It is controlled in synchronous frame of reference with feedforward compensation and a balanced current is generated during asymmetrical faults also. North American grid codes (NA-GCs) are used in modelling the PV plant and it operates at a power factor close to unity [18].

Performance of the distance relay at bus 25 is tested for phase-A-to-ground (AG) and phase-B-to-phase-C-to-ground (BCG) faults created in different conditions and results are provided in Fig. 3. For first two cases, the faults are created at F_1 (at 0.6 pu distance of line 25-2 from Bus-25) with $R_F = 25\Omega$ and 10Ω respectively for two different system conditions. At F_2 an AG fault is created with $R_F = 20\ \Omega$ for the third case (at a distance of 0.1 pu of the line 2-3 from Bus-2) . Lines in the system are protected by distance relay having a standard quadrilateral setting [12] and maximum fault resistance is considered as 60Ω. Results demonstrate clear maloperations of the relay for all the cases with both security and dependability issues. This asks for a new technique to be developed to obtain correct zone-1 decisions in such situations.

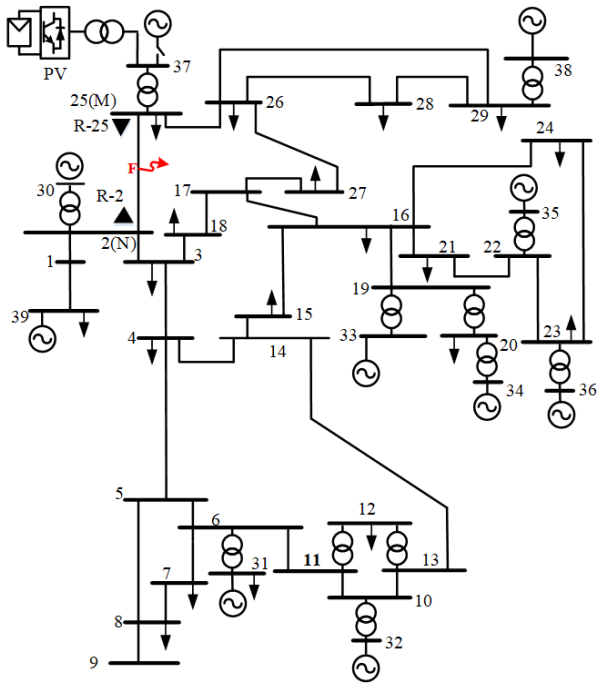

Fig. 2. Modified 39-Bus New England system.

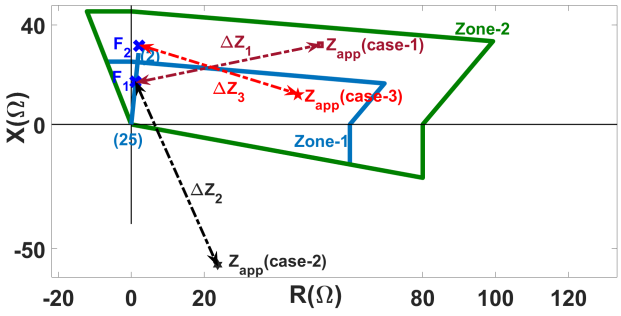

Fig. 3. Maloperation of distance relay in renewable integrated network.

III. Proposed Method

A current source with a parallel impedance at any particular instance is modelled as a voltage source equivalent using source conversion techniques. Using this concept, the two sources in Fig. 1 at bus M in are simplified in Fig. 4, where the equivalent impedance (Z_{SM}) varies with the control operation and renewable penetration level.

Using the polar forms of the phasors, (1) is represented as

$$|Z_{app}|\angle\theta_{app} = x|Z_{1MN}|\angle\theta_{1MN} + \left|\frac{I_F}{I_{RM}}\right| R_F\angle\alpha \quad (2)$$

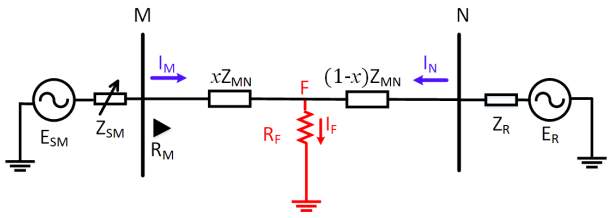

Fig. 4. Simplified two bus equivalent model of a CIRP integrated network.

where,

$$\alpha = arg(I_F) - arg(I_{RM}) \tag{3}$$

(2) can be rearranged as

$$|Z_{app}|\angle(\theta_{app} - \alpha) = x|\,Z_{1MN}|\angle(\theta_{1MN} - \alpha) + \left|\frac{I_F}{I_{RM}}\right| R_F. \tag{4}$$

By equating the both side imaginary parts of (4), (4) is simplified as in (5).

$$|Z_{app}|\sin(\theta_{app} - \alpha) \;= x\,|Z_{1MN}|\sin(\theta_{1MN} - \alpha) \tag{5}$$

Per unit fault distance, x in (5) is obtained as

$$x = \frac{|Z_{app}|\sin(\theta_{app} - \alpha)}{|Z_{1MN}|\sin(\theta_{1MN} - \alpha)}. \tag{6}$$

With a zone-1 reach setting of 80% of the line-MN, a range can be defined as in (7).

$$0 < \frac{|Z_{app}|\sin(\theta_{app} - \alpha)}{|Z_{1MN}|\sin(\theta_{1MN} - \alpha)} < 0.8 \tag{7}$$

From (7), two conditions are derived in (8) for zone-1 faults.

$$\begin{aligned} |Z_{app}|\sin(\theta_{app} - \alpha) \;&> 0 \\ 0.8\,|Z_{1MN}|\sin(\theta_{1MN} - \alpha) &> |Z_{app}|\sin(\theta_{app} - \alpha) \end{aligned} \tag{8}$$

By defining $D_1 = |Z_{app}|\sin(\theta_{app} - \alpha)$ and $D_2 = 0.8\,|Z_{1MN}|\sin(\theta_{1MN} - \alpha)$, the conditions in (8) can be rewritten as in (9).

$$\begin{aligned} D_1 &> 0 \\ D_2 - D_1 &> 0 \end{aligned} \tag{9}$$

All the parameters in (8) except α can be obtained directly using the measurements available at the relay location. The deviation angle α depends on the faulted path current and is determined below for all fault types.

A. For three phase fault

Equivalent model of the renewable integrated system in Fig. 4 during pre-fault and 3-phase fault are shown in Fig. 5 and Fig. 6 respectively. Applying Kirchhoff's law in Fig. 5 and Fig. 6, a pure-fault network model for 3-phase fault can be obtained as in Fig. 7 [4]. Incremental current, $\Delta I_{1(M,N)}$ at each end is obtained as, $\Delta I_{1(M,N)} = I^{fault}_{1(M,N)} - I^{Pre}_{1(M,N)}$. Equivalent source impedances in pre-fault (Z^{Pre}_{1SM}), fault (Z^{fault}_{1SM}) and pure-fault (Z^{pf}_{1SM}) models are different from each other.

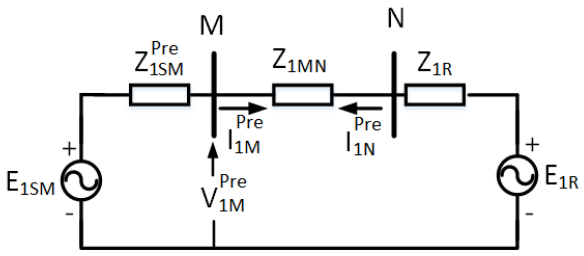

Fig. 5. Equivalent model of a renewable integrated system during pre-fault.

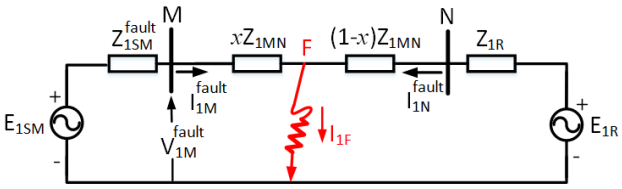

Fig. 6. Equivalent model of a renewable integrated system during fault.

Applying the property of current distribution in Fig. 7, faulted path current (I_{1F}) can be expressed as,

$$I_{1F} = \Delta I_{1M}\left(\frac{Z^{pf}_{1SM} + Z_{1MN} + Z_{1R}}{(1-x)Z_{1MN} + Z_{1R}}\right) \tag{10}$$

Considering the grid to be strong, (10) can be simplified as in (11) [4].

$$I_{1F} \approx \Delta I_{1M}\left(\frac{Z^{pf}_{1SM} + Z_{1MN}}{(1 - x + K_1)Z_{1MN}}\right) \tag{11}$$

Where, $K_1 = \frac{Z_{1G}}{Z_{1MN}}$. With the homogeneity consideration in transmission network, phase angle of I_{1F} is obtained using

$$arg(I_{1F}) = \arg\left(\left(1 + \frac{Z^{pf}_{1SM}}{Z_{1MN}}\right)\Delta I_{1M}\right). \tag{12}$$

Apparent impedance calculated for a 3-phase fault (with phase-A as reference) is given by

$$Z_{app} = \frac{V_{AM}}{I_{AM}} = \frac{V_{1M}}{I_{1M}}. \tag{13}$$

Using (12), α in (3) for a 3-phase fault can be obtained as

$$\alpha_{ABC} = \arg\left(\left(1 + \frac{Z^{pf}_{1SM}}{Z_{1MN}}\right)\Delta I_{1M}\right) - \arg(I^{fault}_{1M}). \tag{14}$$

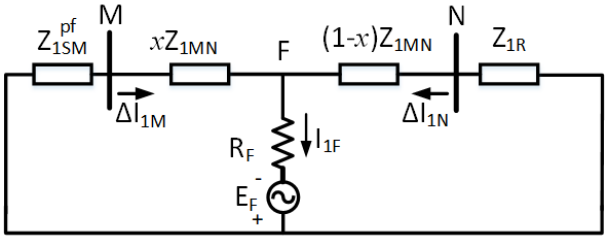

Fig. 7. Pure-fault model of a renewable integrated power network during 3-phase fault.

Z_{1SM}^{pf} in (14) is computed using (15) [4].

$$Z_{1SM}^{pf} = \frac{V_{1M}^{Pre} - V_{1M}^{fault}}{I_{1M}^{fault} - I_{1M}^{Pre}} \tag{15}$$

B. For Phase-A-to-ground Fault

Apparent impedance calculated for phase-A-to-ground (AG) fault is given by

$$Z_{app} = \frac{V_{AM}}{I_{AM} + K_{0L} I_{0M}} \tag{16}$$

K_{0L} is the compensation factor for zero sequence. Faulted path current in such a fault case is I_{1F}, similar to 3-phase fault, as observed from the pure-fault sequence network in Fig. 8.

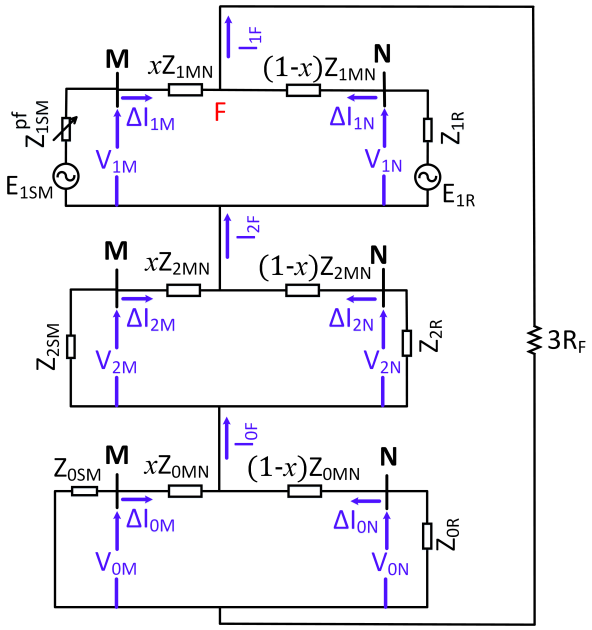

Fig. 8. Pure fault sequence network for AG fault.

Thus α for AG fault can be estimated using (17).

$$\alpha_{AG} = \arg\left(\left(1 + \frac{Z_{1SM}^{pf}}{Z_{1MN}}\right)\Delta I_{1M}\right) - \arg(I_{AM}^{fault} + K_{0L} I_{0M}^{fault}) \tag{17}$$

C. For Phase B-to-Phase C fault

Apparent impedance calculated for phase B-to-phase C (BC) fault is given by

$$Z_{app} = \frac{V_{BM} - V_{CM}}{I_{BM} - I_{CM}} = \frac{V_{1M} - V_{2M}}{I_{1M} - I_{2M}} \tag{18}$$

Using the pure-fault network in Fig. 9, the faulted path current for BC fault is given as,

$$I_F = I_{1F} - I_{2F} = 2I_{1F}. \tag{19}$$

Thus α for a BC fault can be computed using (20).

$$\alpha_{BC} = \arg\left(\left(1 + \frac{Z_{1SM}^{pf}}{Z_{1MN}}\right)\Delta I_{1M}\right) - \arg(I_{1M}^{fault} - I_{2M}^{fault}) \tag{20}$$

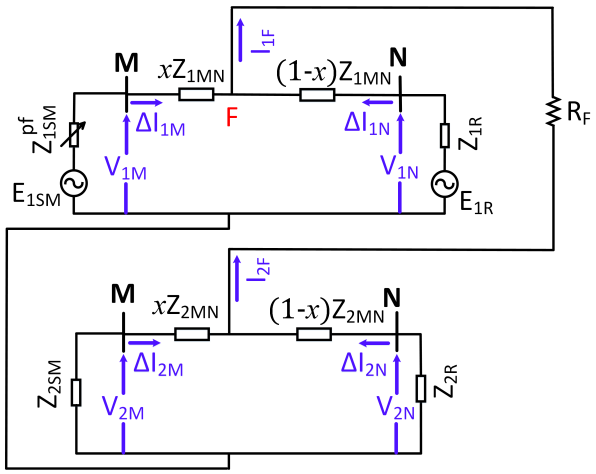

Fig. 9. Pure fault sequence network for BC fault.

D. For Phase B-to-Phase C-to-ground fault

Apparent impedance for BCG fault are calculated similar to BC fault. Using the pure-fault network in Fig. 10, the current in faulted path for BCG fault is given as,

$$I_F = I_{1F} - I_{2F}. \tag{21}$$

α for a BCG can be estimated using (22) [4].

$$\alpha_{BCG} = \arg\left(\left(1 + \frac{Z_{1SM}^{pf}}{Z_{1MN}}\right)\Delta I_{1M} - \left(1 + \frac{Z_{2SM}^{pf}}{Z_{1MN}}\right)\Delta I_{2M}\right) - \arg(I_{1M}^{fault} - I_{2M}^{fault}) \tag{22}$$

where the negative sequence pure-fault source impedance (Z_{2SM}^{pf}) can be obtained as

$$Z_{2SP}^{pf} = -\frac{V_{2M}^{fault}}{I_{2M}^{fault}}. \tag{23}$$

IV. Results

Proposed method is assessed for different fault conditions for the relay at bus 25 as shown in Fig. 2 for its performance.

A. Detection of Zone-1 fault, when seen in Zone-2 by conventional distance relay

On the line 25-2, a distance of 0.6 pu of from Bus-25 an AG Fault is created with $R_F = 25\Omega$. Result in Fig. 11 demonstrates that the apparent impedance computed by the conventional distance protection relay at bus 25 is found in zone-2 and fails to provide instantaneous protection decision even for the zone-1 fault. Where as, the proposed method computes two indices following fault detection. As shown in Fig. 12 positive values of both D_1 and $(D_2 - D_1)$ satisfy the criteria in (9). Thus the proposed method indicates a zone-1 fault and ensures the desired instantaneous protection.

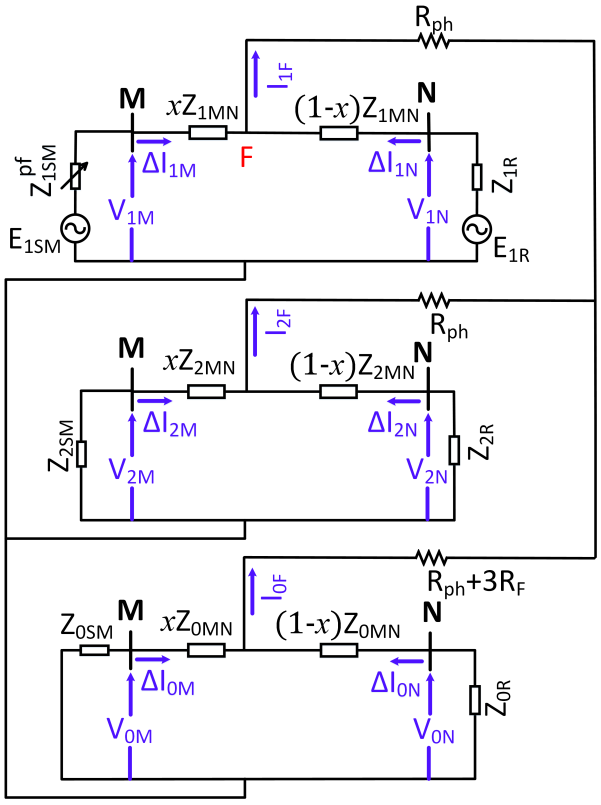

Fig. 10. Pure fault sequence network for BCG fault.

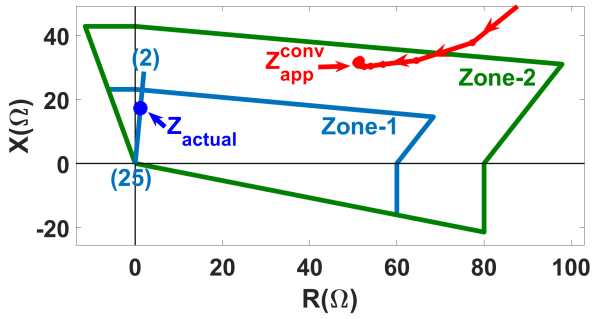

Fig. 11. Identification of zone-1 fault in zone-2 by the conventional distance relay.

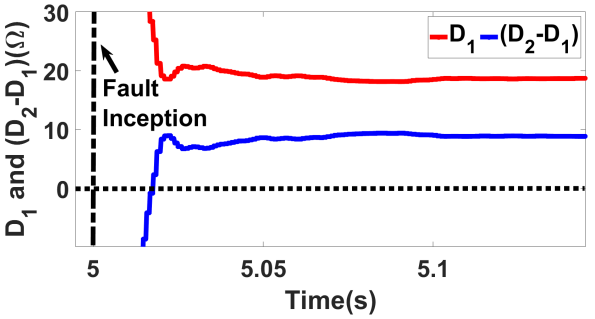

Fig. 12. Performance of the proposed method in identifying zone-1 fault.

B. Detection of Zone-1 fault, when not seen in zone boundaries by conventional distance relay

For a situation, the line 25 -26 is considered to be out of operation. On the line 25-2, a distance of 0.6 pu of from Bus-25 a BCG fault is created with $R_F = 10\ \Omega$. Fig. 13 demonstrates that the conventional distance relay at bus 25 does not find the apparent impedance in both zone-1 and zone-2 boundaries and fails to detect the fault. Even for such a situation Results in Fig. 14 confirms the correctness of the proposed method. This shows the strength of the method.

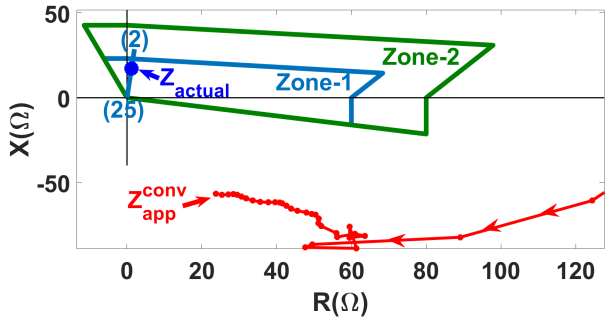

Fig. 13. Maloperation of conventional distance relay for zone-1 fault.

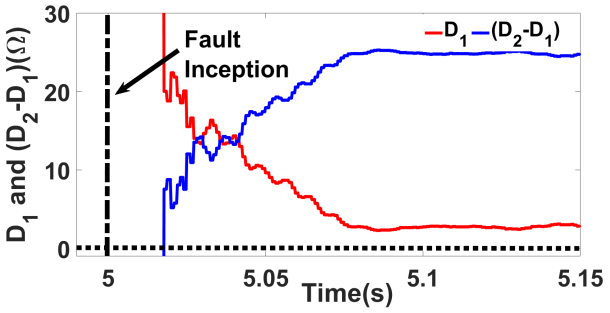

Fig. 14. Performance of the proposed method for zone-1 fault.

C. Security against out-of-zone faults, when seen in Zone-1 by conventional distance relay

At a distance of 0.1 pu of the line 2-3 from Bus-2 in a different loading condition, an AG fault is created with $R_F = 20\ \Omega$. From Fig. 15, it can be shown that the computed impedance of conventional distance relay at bus 25 is found in zone-1 even for such a zone-2 fault and issues an unintentional trip signal for the circuit breaker, Whereas the proposed method computes the indices, as shown in Fig. 16. Positive value of D_1 indicates a forward fault, whereas the negative value of $(D_2 - D_1)$ confirms the fault not to be in zone-1. Thus the proposed method prevents the instantaneous tripping of conventional distance relay and maintains security against out-of-zone faults.

V. Conclusion

The fault characteristics of the power network are modulated by Control schemes linked with the renewable source,

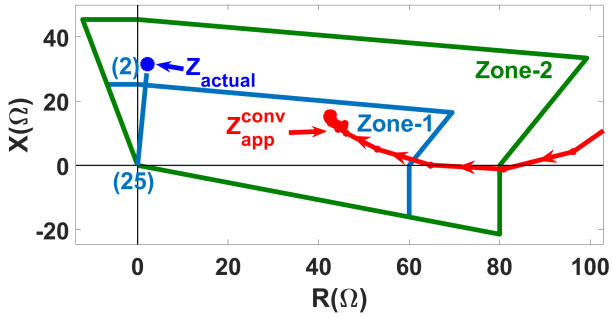

Fig. 15. Identification of zone-2 fault in zone-1 by the conventional distance relay.

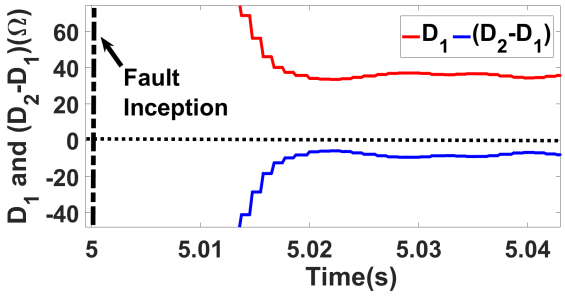

Fig. 16. Performance of the proposed method in identifying out-of-zone fault.

affecting the performance of the distance relay. Both dependability and security issues are observed for conventional distance relays with such connectivity, especially for high fault resistance faults. A new method for protection method is to ensure correct zone-1 operation of distance relay. The method calculates two indices by determining the faulted path current angle and is independent of control schemes in the renewable plants. The improved performance of the proposed method is demonstrated for both zone-1 and zone-2 faults in different situations. Analysing the performances of proposed method and conventional distance relaying schemes displays the strength of the method suggested.

REFERENCES

[1] "Guidelines for implementation of scheme for setting up of 750 MW grid-connected solar PV power projects under batch-1," Jawharlal Nehru National Solar Mission, Ministry of New and Renewable Energy, New Delhi, India, Tech. Rep., October 2013, [Online].

[2] Hasanien, Hany M. "An adaptive control strategy for low voltage ride through capability enhancement of grid-connected photovoltaic power plants." *IEEE Tran., on power syst.* 31, no. 4 (2015): 3230-3237.

[3] Shuai, Zhikang, et al. "Fault analysis of inverter-interfaced distributed generators with different control schemes." *IEEE Tran., on Power Del.* 33.3 (2017): 1223-1235.

[4] Paladhi, Subhadeep, and Ashok Kumar Pradhan. "Adaptive distance protection for lines connecting converter-interfaced renewable plants." *IEEE Journal of Emerging and Selected Topics in Power Electron.* (2020).

[5] Paladhi, Subhadeep, and Ashok Kumar Pradhan. "Adaptive fault type classification for transmission network connecting converter-interfaced renewable plants." *IEEE Systems* Journal (2020).

[6] Pradhan, A. K., and Gza Joos. "Adaptive distance relay setting for lines connecting wind farms." *IEEE Tran., on Energy Conversion* 22, no. 1 (2007): 206-213.

[7] Banaiemoqadam, Amin, Ali Hooshyar, and Maher A. Azzouz. "A control-based solution for distance protection of lines connected to converter-interfaced sources during asymmetrical faults." *IEEE Tran., on Power Deliv.* 35, no. 3 (2019): 1455-1466.

[8] Paladhi, Subhadeep, and Ashok Kumar Pradhan. "Adaptive zone-1 setting following structural and operational changes in power system." *IEEE Tran., on Power Deliv.* 33, no. 2 (2017): 560-569.

[9] Paladhi, Subhadeep, and Ashok Kumar Pradhan. "Resilient protection scheme preserving system integrity during stressed condition." *IET Gen., Tran. & Dist.* 13, no. 14 (2019): 3188-3194.

[10] Thompson, Michael J., and Amit Somani. "A tutorial on calculating source impedance ratios for determining line length." In 2015 *68th Annual Conference for Protective Relay Engineers*, pp. 833-841. IEEE, 2015.

[11] Alstom, "Network protection and automation guide," Tech. Rep. 978-0-9568678-0-3, May 2011.

[12] Liang, Yingyu, et al. "A novel fault impedance calculation method for distance protection against fault resistance." *IEEE Tran., on Power Deliv.* 35.1 (2019): 396-407.

[13] Ma, Jing, et al. "An adaptive distance protection scheme based on the voltage drop equation." *IEEE Tran., on Power Deliv.* 30.4 (2015): 1931-1940.

[14] Hooshyar, Ali, Maher A. Azzouz, and Ehab F. El-Saadany. "Distance protection of lines emanating from full-scale converter-interfaced renewable energy power plants—Part II: Solution description and evaluation." *IEEE Tran., on Power Deliv.* 30, no. 4 (2014): 1781-1791.

[15] Fang, Yu, et al. "Impact of inverter-interfaced renewable energy generators on distance protection and an improved scheme." *IEEE Tran., on Indus. Electron.* 66.9 (2018): 7078-7088.

[16] Hiskens, Ian. "IEEE PES task force on benchmark systems for stability controls." Technical Report (2013).

[17] Loutan, Clyde, et al. *Demonstration of essential reliability services by a 300-MW solar photovoltaic power plant*. No. NREL/TP-5D00-67799. National Renewable Energy Lab.(NREL), Golden, CO (United States), 2017.

[18] Hooshyar, Ali, Ehab F. El-Saadany, and Majid Sanaye-Pasand. "Fault type classification in microgrids including photovoltaic DGs." *IEEE Tran., on Smart Grid* 7, no. 5 (2015): 2218-2229.